

Journal of Materials Chemistry C

Accepted Manuscript



This is an *Accepted Manuscript*, which has been through the Royal Society of Chemistry peer review process and has been accepted for publication.

Accepted Manuscripts are published online shortly after acceptance, before technical editing, formatting and proof reading. Using this free service, authors can make their results available to the community, in citable form, before we publish the edited article. We will replace this *Accepted Manuscript* with the edited and formatted *Advance Article* as soon as it is available.

You can find more information about *Accepted Manuscripts* in the [Information for Authors](#).

Please note that technical editing may introduce minor changes to the text and/or graphics, which may alter content. The journal's standard [Terms & Conditions](#) and the [Ethical guidelines](#) still apply. In no event shall the Royal Society of Chemistry be held responsible for any errors or omissions in this *Accepted Manuscript* or any consequences arising from the use of any information it contains.

Fabrication of Periodic Nanoparticle Clusters Using Soft Lithographic Template

Cite this: DOI: 10.1039/x0xx00000x

Dae Seok Kim,^a Apiradee Honglawan,^b Kyungnam Kim,^c Mun Ho Kim,^d Sohee Jeong,^{ce} Shu Yang,^{bf} Dong Ki Yoon^{a*}

Received 00th January 2015,

Accepted 00th January 2015

DOI: 10.1039/x0xx00000x

www.rsc.org/

A novel fabrication method is developed for preparation of periodic array of nanoparticle clusters (NPCs) using sublimable liquid crystal (LC) material. The defect structures of the LC film provide the specific topographical confinement to trap nanoparticles (NPs) and assemble the NPs to generate NPCs during the thermal annealing. This system shows simple regulation of the size of NPCs by varying concentration of NP-suspension. Additionally, an illuminating system using quantum dots (QDs) is fabricated by the manipulation method reported here.

NPs that self-assemble into ordered nanostructures present unusual structural and opto-electric characteristics¹⁻³. Especially, creation of a large area array of NPCs is one of the most important interdisciplinary topics in current materials science and optoelectronics for the manipulation of tuneable photonic devices. To date, many assembling methods, including drying oil-emulsion template in water, electrostatic assembly, chemical vapour deposition and template assisted assembly have been tried to control the ordering and orientation of NPCs³⁻⁶. However, achieving a well-ordered array of NPCs is still a complex and expensive process^{7,8}. One of the promising methods to assembly NPs is using self-organization process in LC medium.⁹ Herein, we demonstrate fabrication of periodic array of NPCs over a large area using a sublimable LC material. This is mainly governed by two factors: the topographical LC dimple structures to confine the NPs and the sublimation–reconstruction phenomenon of small molecular weight LC molecules to generate NPC array. The number of NPs in a NPC, which is important for the optoelectronic properties, is controlled by the concentration of NP suspension. We extend the method to create a hexagonal array of QDs for fluorescent display, where the symmetry of the clusters is determined by highly periodic defect array of toric focal conic domains (TFCDs). We believe that the toolkit presented here is universal and will find uses in other new applications involving assembly of NPs or NPCs. Highly periodic dimple structures, the TFCDs of smectic A LC phase (SmA), are formed by the antagonistic surface anchoring;

planar anchoring on the solid substrate and homeotropic anchoring at the air/LC interface¹⁰. It was shown that TFCDs can be used as lithographic tools to address particles in the line defect of the dimple sites⁹. However, after the assembly of particles, LCs remain in the matrix. For many practical applications, it will be desirable to remove the assembling LCs. It has been shown that like ice in winter, the small molecular weight LC molecules exhibit the sublimation and reconstruction properties that enable the TFCDs at a micron scale to transform into dome-like TFCDs with hemicylinders at the nanometre scale during the thermal annealing process^{11,12}.

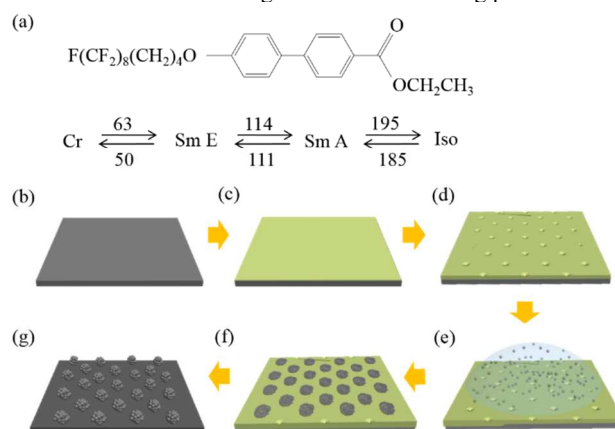


Fig. 1 Liquid crystal material and schematic representation of the strategy used to fabricate NPCs array. (a) The structures, phases, and transition temperatures of the rod type LC material, **Y002** (all temperatures are in degrees of Celsius). (b) A clean pristine Si (100) wafer is prepared. (c) **Y002** is placed on the Si wafer and then heated above the isotropic temperature (~ 200 °C). (d) TFCD array is formed on cooling from the isotropic state to SmA (~ 160 °C). (e) The NP suspension is spread and spin-coated on the TFCD array. (f) NPs are spontaneously aggregated at the dimple region of the TFCD array. (g) NPCs array is generated with hexagonal symmetry after the thermal

To create the NPC array using sublimable LC material, we first prepare a rod-type semifluorinated LC molecule, **Y002** (Fig. 1a),¹⁰ which undergoes transitions from isotropic state to SmA phase, smectic E phase (SmE) and to crystalline phase from 195 °C to room temperature and has the thermal sublimating property^{11,12}. As a proof-of-concept, we also synthesized multidimensional NPs, including fluorinated silica NPs (F-SiO₂; diameter (d) ~ 100 nm), and QDs (CdSe/CdS/ZnS, 4-5 nm in diameter) according to literature^{13,14}. As illustrated in Fig. 1b to g, the powder sample, **Y002** is first put on a clean Si (100) wafer with planar anchoring, followed by heating up to the isotropic temperature to spread the LC sample with a thickness of ~10 μm. After cooling to room temperature, TFCDs with dimple structures are spontaneously generated on top, typically a few μm in width and hundreds nanometers in depth, which can be varied by the LC film thickness¹⁵. These topographical dimples can grab or confine the particles similar to the photolithographically generated hole patterns⁶. To use these dimple structures as a template for the NPCs array, 0.01 wt% suspension of F-SiO₂ NP in Novec 7300 (3 M) is spin coated (2,000 rpm, 15 s) on the TFCDs film (Fig. 1e). As the sample is dried via solvent evaporation, the NPs aggregate irregularly at each dimple site (Fig. 1f). When annealed at 160 °C, the smectic layers of TFCDs are slowly removed layer by layer as a function of time. In particular, the layers near the dimple region sublime slower than other sites and become spherically reoriented with F-SiO₂ NPs at the same time. Finally, a hexagonal array of NPCs is generated (Fig. 1g) after 4 h-thermal annealing. This fabrication process is directly investigated by depolarized reflected light microscopy (DRLM) and scanning electron microscopy (SEM). Despite the existence of a layer of F-SiO₂ NPs on top, the hexagonal array of TFCDs shows typical Maltese cross patterns in the DRLM images at room temperature (Fig. 2a), indicating that the molecular director is radially orientated at the bottom of substrate. The corresponding SEM image confirms

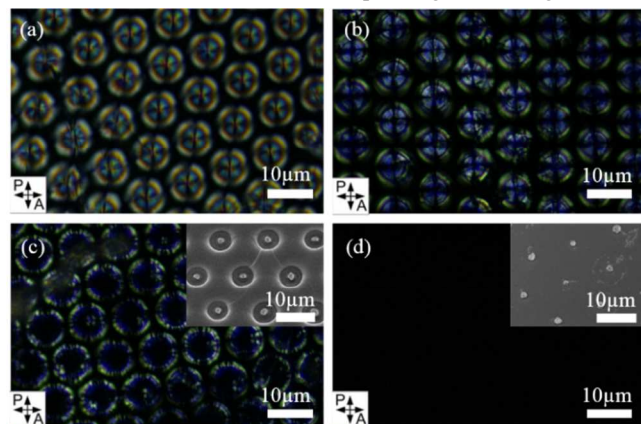


Fig. 2 DRLM with cross-polarizers and SEM images of the TFCDs top-coated by F-SiO₂ NPs during thermal annealing at 160 °C. (a) The initial state of the TFCDs showing Maltese cross patterns. (b, c) The images of TFCDs are taken after 1 and 2 h annealing, respectively. The molecular arrangement at the micron scale does not change compared to the initial state. (d) The totally dark image is observed after all the LC molecules were removed by sublimation. The insets of (c, d) are the corresponding SEM images, respectively.

that the micron-scale TFCDs are not distorted by NPs (Fig. 3a).

After heating and dwelling the sample at 160 °C for 1 h, the LC molecules are slowly sublimed from the top-surface of the sample, gathering NPs, thus forming a NPC in the dimple region (Fig. 3b). This selective gathering behaviour is consistent with the characteristics of the sublimable LC molecules, which sublimed

much slower (indicated by thin and thick arrows in Fig. 3b,c) in the dimple regions than the peripheral area of the dimple, as illustrated in Fig. 3b-c. The different sublimation rates in the dimple and the other area of the TFCD are resulted from a combination effect of surface tension and surface orientational interactions.¹¹ As the thermal annealing proceeds, the more air/LC interface is exposed to induce the homeotropic alignment of LC molecules, which means the smectic layers parallel aligned with the air/LC interface. In this process, the antagonistic alignment of LC molecules in the line defect, the dimple site and the other place of the TFCD makes the dome-like structure because the molecules in the line defect has the bigger resistance compared the edge of the TFCD for the thermal sublimation.¹¹ This interesting behaviour reveals differently when

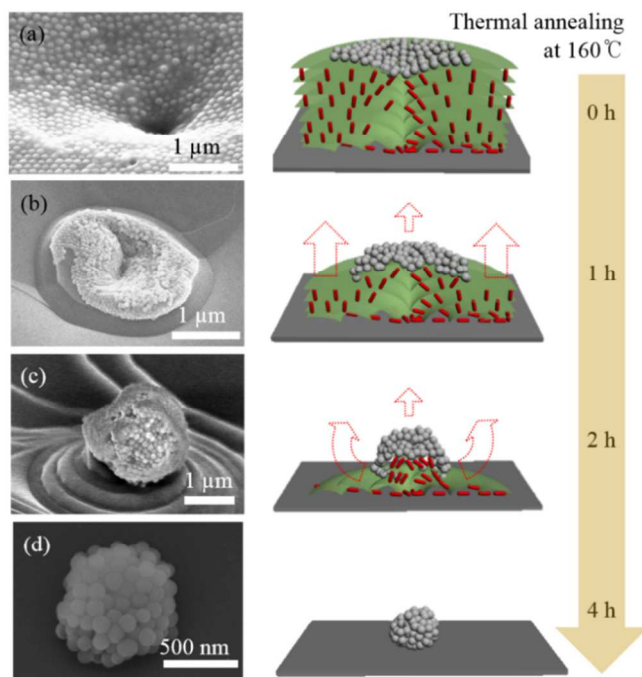


Fig. 3 SEM images and the corresponding illustrations of the NPCs during the thermal annealing. (a) SEM image of the initial state, showing the relatively flat arrangement of F-SiO₂ particles on TFCD. (b, c) As time goes at ~160 °C, smectic LC layers are sublimed and partially reconstructed to spherically address NPs at the dimple region of the TFCD. (d) NPs remain at the dimple position of TFCD after all the LC materials are sublimed. A series of illustrations show that the layers of the dimple region are mixed with NPs, whereas the interconnecting layers between dimples were gradually removed during the thermal annealing. Finally, the NPs accumulate together to form a NPC on the substrate without the LC material. The wider arrow means the faster subliming rate in (b, c).

the F-SiO₂ NPs are placed on top of the TFCD.

The macroscopic reorientation of LC molecules is not found although the NPs migrate to the top-surface of TFCDs during the thermal annealing (Fig. 2b,c). This is due to the small elastic energy of TFCD not to overcome surface energy that can reorient LC molecules to satisfy the planar anchoring of NPs at LC/air interface¹⁶. A few hundreds nm-sized concentric ring-patterns are generated, as the total thickness of TFCDs is gradually reduced with increasing thermal annealing time at the SmA phase (160 °C) for ~ 2 h (Fig. 3c)^{11,12}. Topographically, the centre of the ring patterns become higher while the surroundings are sublimed away, resulting in NPC protrusion in the centre of the ring-patterns (Fig. 3c). Most of the NPs are gathered at the dimple site of TFCD to form a NPC (Fig. 3c), showing a diameter of ~2 μm in the hexagonal array (inset

of Fig. 2c and Fig. 3c). After 4 h-thermal annealing process, all the LC materials are gone, leaving only the spherical aggregates of F-SiO₂ NPs at the original dimple site of TFCD (Fig. 3d). This is also observed in the DRLM image, showing no birefringence (Fig. 2d), indicating complete removal of the LC molecules. The size of NPC is reduced to ~ 800 nm, and SEM image clearly shows a highly-ordered NPCs array (inset of Fig. 2d and Fig. 3d) over a large area (~ 500 × 500 μm²)

The roles of F-SiO₂ NPs relevant to clustering of NPs are as follows: (i) Spread NPs on the TFCDs reduce the sublimating rate of LC material especially at the dimple region as shown in Fig. 3b,c. The more NPs are gathered in the dimple region with increasing thermal annealing time, which hinder the direct contact of LCs with air boundary, the less LC molecules being removed in this area. As a consequence, the LC molecules in the peripheral region of TFCDs without NPs sublime much faster where molecules are vertically aligned. (ii) Top-coated NPs locally induce planar anchoring to Y002 molecules¹⁶, leading to the intercalation of LC molecules among the NPs to form a spherical NPC during the thermal annealing. Supporting this is the reduced NPC size from ~2 μm (2 h) to ~800 nm (4 h) as shown in Fig. 3c and d, respectively.

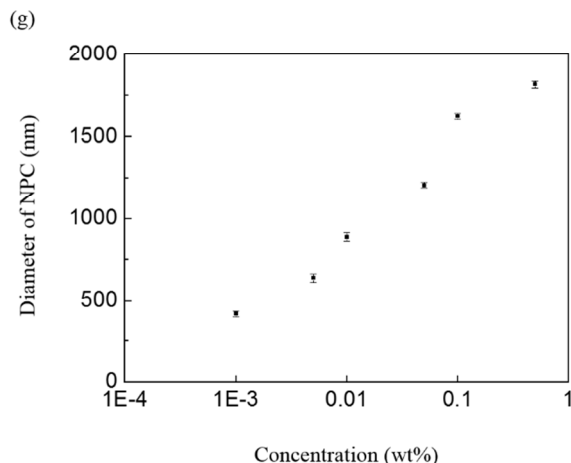
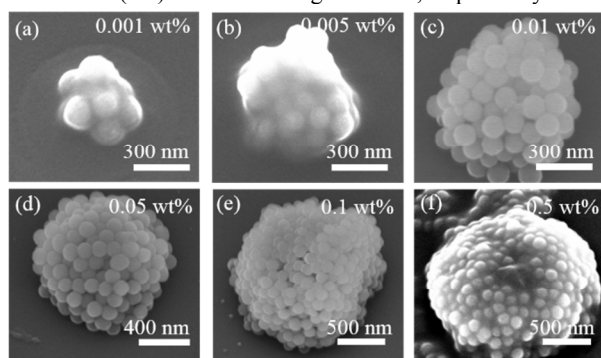


Fig. 4 SEM images of NPCs with varied concentrations of the NP suspensions and its relationship. A series of SEM images of NPC using varied concentrated suspension of NPs of (a) 0.001 wt%, (b) 0.005 wt%, (c) 0.01 wt%, (d) 0.05 wt%, and (e) 0.1 wt%, (f) 0.5 wt%. (g) The plot quantitatively shows increase of the size of the NPCs as a function of concentration of NP suspension. In this plot, the x-axis, concentration is a log-scale, while the y-axis is the diameter of NPCs.

We then investigated a control of the NPC size by varying the concentration of NP-suspension (Fig. 4). As the concentration varies from 0.001 wt% to 0.5 wt%, the size of the NPC also varies from 400 nm to 1.8 μm in diameter, meaning the number of NPs in a

cluster might be commensurate from ~64 to ~6000. At a concentration as low as 0.0001 wt%, we observe a single or dimer form of NPs, meaning that our building block, F-SiO₂ NP has a critical size forming NPC around this concentration. On the contrary, at 1 wt% suspension, relatively irregular NPCs are obtained and NPs are not well-gathered in the dimple region of TFCDs. Instead, they spread over the substrate after thermal annealing. This tendency can be also found in NPC made from 0.5 wt% suspension, showing the irregular aggregation in the background (Fig. 4f). Clustering of NPs shown in Fig. 4g can be qualitatively understood by a simple growth pattern⁷. This size tenability is very important for the photonic and optoelectronic applications^{17,18}, where the optoelectronic properties of each NPC can be varied with a degree of the aggregation of NPs.

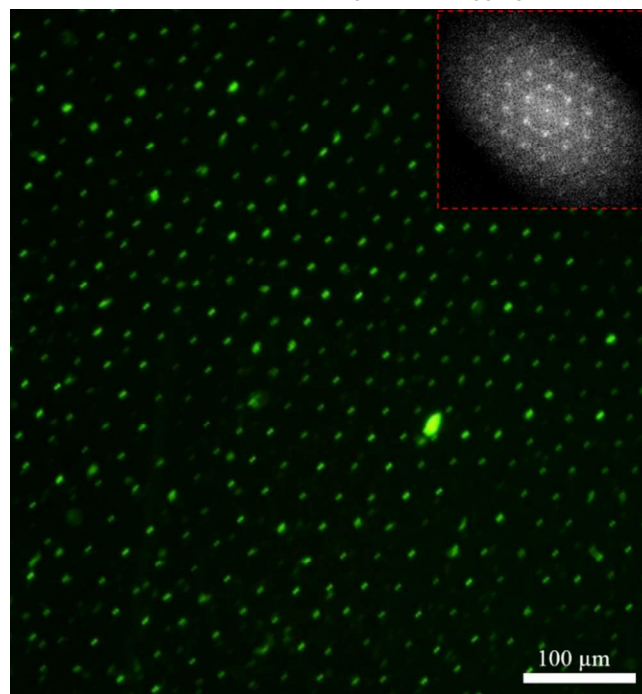


Fig. 5 The QD clusters based illumination. A fluorescent microscopy image of the QD clusters in the hexagonal array. Inset is 2 dimensional fast Fourier transform.

To demonstrate the versatility of our method, we extend the study to manipulate the illumination from QDs. The semiconductor QDs present size-tuneable optical properties arising from the quantum confinement effects, which has been a very attractive for display devices^{19,20}. There have been many studies to fabricate QD array, including dewetting method using a mold, inkjet printing, solution-based nucleation and growth and transfer printing²¹⁻²⁴.

Nevertheless, it often requires pre-patterning the templates, use of expensive equipment, and complex processing steps. Here, in order to realize the illumination, we only need sublimable LC materials and CdSe/CdS/ZnS QDs with an excitation maximum at ~450 nm (blue) and emission at ~550 nm (green). As shown in the fluorescent microscopy image (Fig. 5), a hexagonal array of QD cluster is observed over a large area (~ 500 × 500 μm²) in ~4 h via spontaneous assembly of QDs and LC. The fast Fourier transform (FFT) (inset in Fig. 5) clearly shows the well-ordered QD cluster arrays in a hexagonal symmetry. Moreover, it is possible to realize various types of arrays of NPCs including QD-clusters by using the topographical confinement of LCs^{10,25-28}.

Conclusions

We have developed a simple method to fabricate periodic array of NPCs using sublimable LCs. This process is mainly governed by the thermal annealing condition to control the sublimation rate and reconstruction phenomenon of sublimable LCs. The dimples of TFCDs provide important topographical sites to trap and assemble NPs to make NPCs during the thermal annealing. The NPs in turn slow down the sublimation of LCs in the dimple regions. We also show that the size of NPCs can be conveniently controlled by varying the concentration of NP-suspension. As a proof-of-concept, an illuminating system consisting of a hexagonal array of QDs is fabricated. The self-assembly approach demonstrated here can be applied to the flexible substrate and will offer a new universal platform to fabricate and explore optoelectronic devices via bottom-up approaches.

Acknowledgements

This study was supported by the grant from the National Research Foundation (NRF), funded by the Korean Government (2014M3C1A3052537, 2012M3A7B4049802, 2014S1A2A2027911, and 2014M1A8A1049303). S.Y. and A.H. acknowledge support by the National Science Foundation (NSF) MRSEC grant, DMR1120901. K. K and S. J. were partially supported by Basic Research Fund from KIMM.

Notes and references

^a Graduate School of Nanoscience and Technology and KINC, KAIST, Daejeon 305-701, Republic of Korea

^b Department of Chemical and Biomolecular Engineering, University of Pennsylvania, PA 19104, USA

^c Nanomechanical Systems Research Division, Korea Institute of Machinery and Materials, Daejeon, 305-343, Republic of Korea

^d Department of Polymer Engineering, Pukyong National University, Pusan, 608-739, Republic of Korea

^e Department of Nano Mechatronics, University of Science and Technology, Daejeon, 305-350, Republic of Korea

^f Department of Materials Science & Engineering, University of Pennsylvania, 3231 Walnut Street, PA 19104, USA

*Corresponding Author's E-mail : nandk@kaist.ac.kr

† *Materials and procedures*: **Y002**, F-SiO₂ NPs (d ~ 100 nm), and QDs (CdSe/CdS/ZnS, 4 ~ 5 nm in diameter) were synthesized as reported previously with some modifications^{9,12,13}. Si wafer was cleaned by rinsing with acetone and ethanol to remove organic and inorganic impurities, and then dried by N₂ gas. To introduce planar anchoring at the bottom substrate, 1 wt% polyethylene imide (Sigma Aldrich) solution was spin-coated on the cleaned Si wafer and baked at 90 °C for 30 min. Then **Y002** powder was placed on the substrate and heated to the isotropic temperature (~200 °C) on a heating stage (LINKAM LTS350) controlled by a temperature controller (LINKAM TMS94), and cooled down to room temperature to form the TFCDs. To form NPCs, F-SiO₂ NPs and CdSe/CdS/ZnS QDs were spin coated on the TFCDs and maintained at 160 °C for 1, 2, and 4 h, respectively, to observe the sequential changes of the clusters.

Characterization by DRLM, SEM, and FM

The clustering NPs was directly imaged using DRLM (LV100POL, Nikon) and field-emission SEM (FE-SEM, Hitachi, S-4800). The fluorescent image of QD-clusters array was obtained by Epi-Fluorescence microscopy (LV-UDM, Nikon). The excitation and emission wavelengths were in the range 440–460 nm and 540–560 nm, respectively.

- S. M. Spillane, T. J. Kippenberg, K. J. Vahala, *Nature* 2002, **415**, 621.
- J. A. Fan, C. Wu, K. Bao, J. Bao, R. Bardhan, N. J. Halas, V. N. Manoharan, P. Nordlander, G. Shvets, F. Capasso, *Science* 2010, **328**, 1135.
- J. Lacava, P. Born, T. Kraus, *Nano Lett.* 2012, **12**, 3279.
- F. L. Yap, P. Thoniyot, S. Krishnan, S. Krishnamoorthy, *ACS Nano* 2012, **6**, 2056.
- A. Valsesia, P. Colpo, T. Mezzani, F. Bretagnol, M. Lejeune, F. Rossi, A. Bouma, M. G. Parajo, *Adv. Funct. Mater.* 2006, **16**, 1242.
- Y. Xia, Y. Yin, Y. Lu, J. McLellan, *Adv. Funct. Mater.* 2003, **13**, 907.
- B. Yan, A. Yhubagere, W. R. Premasiri, L. D. Ziegler, L. D. Negro, B. M. Reinhard, *ACS Nano* 2009, **3**, 1190.
- L. Gunnarsson, J. E. Bjerneld, H. Xu, S. Petronis, B. Kasemo, M. Kall, *Appl. Phys. Lett.* 2001, **78**, 802.
- C. Blanc, D. Coursault, E. Lacaze, *Liquid Crystal Review* 2013, **1**, 83.
- D. K. Yoon, M. C. Choi, Y. H. Kim, M. W. Kim, O. D. Lavrentovich, H. T. Jung, *Nat. Mater.* 2007, **6**, 866.
- D. K. Yoon, Y. H. Kim, D. S. Kim, O. S. Oh, I. I. Smalyukh, N. A. Clark, H. T. Jung, *Proc. Natl. Acad. Sci. U. S. A.* 2013, **110**, 19263.
- D. S. Kim, Y. J. Cha, H. Kim, M. H. Kim, Y. H. Kim, D. K. Yoon, *RSC advances* 2014, **4**, 26946.
- L. Xu, R. G. Karunakara, J. Guo, S. Yang, *ACS Appl. Mater. Interfaces.* 2012, **4**, 1118.
- K. Kim, J. Y. Woo, S. Jeong, C. S. Han, *Adv. Mater.* 2011, **23**, 911.
- Y. H. Kim, D. K. Yoon, M. C. Choi, H. S. Jeong, M. W. Kim, O. D. Lavrentovich, H. T. Jung, *Langmuir* 2009, **25**, 1685.
- D. A. Beller, M. A. Gharbi, A. Honglawan, K. J. Stebe, S. Yang, R. D. Kamien, *Phys. Rev. X* 2013, **3**, 041026-1.
- F. Kretschmer, F. Kretschmer, M. Fruhnert, R. Geiss, U. Mansfeld, C. Hoppener, S. Hoepfener, C. Rockstuhl, T. Pertsch, U. S. Schubert, *J. Mater. Chem. C* 2014, **2**, 6415.
- R. Philip, P. Chantharasupawong, H. Qian, R. Jin, J. Thomas, *Nano Lett.* 2012, **12**, 4661.
- J. Lim, S. Jun, E. Jang, H. Baik, H. Kim, J. Cho, *Adv. Mater.* 2007, **19**, 1927.
- E. Jang, S. Jun, H. Jang, J. Lim, B. Kim, Y. Kim, *Adv. Mater.* 2010, **22**, 3076.
- W. Cheng, N. Park, M. T. Walter, M. R. Hartman, D. Luo, *Nature Nanotech.* 2008, **3**, 682.
- V. Wood, M. J. Panzer, J. Chen, M. S. Bradley, J. E. Halpert, M. G. Bawendi, V. Bulovic, *Adv. Mater.* 2009, **21**, 2151.
- C. B. Murray, C. R. Kagan, M. G. Bawendi, *Annu. Rev. Mater. Sci.* 2000, **30**, 545.
- T. H. Kim, C. B. Murray, C. R. Kagan, M. G. Bawendi, *Nat. Photon.* 2011, **5**, 176.
- A. Honglawan, D. A. Beller, M. Cavallaro, R. D. Kamien, K. J. Stebe, S. Yang, *Adv. Mater.* 2011, **23**, 5519.
- A. Honglawan, D. A. Beller, M. Cavallaro, R. D. Kamien, K. J. Stebe, S. Yang, *Proc. Natl. Acad. Sci. U. S. A.* 2013, **110**, 34.

Journal Name

- 27 B. Zappone, C. Meyer, L. Bruno, E. Lacaze, *Soft Matter* 2012, **8**, 4318.
- 28 T. Ohzono, Y. Takenaka, J. I. Fukuda, *Soft Matter* 2012, **8**, 6438.